Citation: Molecular Therapy — Methods & Clinical Development (2014) **1,** 14023; doi:10.1038/mtm.2014.23

www.nature.com/mtm

ARTICLE

Prevention of adverse events of interferon γ gene therapy by gene delivery of interferon γ-heparin-binding domain fusion protein in mice

Mitsuru Ando[1], Yuki Takahashi[1], Takuma Yamashita[1], Mai Fujimoto[1], Makiya Nishikawa[1], Yoshihiko Watanabe[2] and Yoshinobu Takakura[1]

Sustained gene delivery of interferon (IFN) γ can be an effective treatment, but our previous study showed high levels of IFNγ-induced adverse events, including the loss of body weight. These unwanted events could be reduced by target-specific delivery of IFNγ after *in vivo* gene transfer. To achieve this, we selected the heparin-binding domain (HBD) of extracellular superoxide dismutase as a molecule to anchor IFNγ to the cell surface. We designed three IFNγ derivatives, IFNγ-HBD_1, IFNγ-HBD_2, and IFNγ-HBD_3, each of which had 1, 2, or 3 HBDs, respectively. Each plasmid-encoding fusion proteins was delivered to the liver, a model target in this study, by hydrodynamic tail vein injection. The serum concentration of IFNγ-HBD_2 and IFNγ-HBD_3 after gene delivery was lower than that of IFNγ or IFNγ-HBD_1. Gene delivery of IFNγ-HBD_2, but not of IFNγ-HBD_3, effectively increased the mRNA expression of IFNγ-inducible genes in the liver, suggesting liver-specific distribution of IFNγ-HBD_2. Gene delivery of IFNγ-HBD_2-suppressed tumor growth in the liver as efficiently as that of IFNγ with much less symptoms of adverse effects. These results indicate that the adverse events of IFNγ gene transfer can be prevented by gene delivery of IFNγ-HBD_2, a fusion protein with high cell surface affinity.

Molecular Therapy — Methods & Clinical Development (2014) **1**, 14023; doi:10.1038/mtm.2014.23; published online 18 June 2014

INTRODUCTION

Interferon (IFN)γ is a type II IFN that exhibits a variety of biological activities, such as antiviral activity, antitumor activity, and regulatory functions on the immune system.[1–5] IFNγ is expected to be useful as a therapeutic agent to treat a variety of diseases, such as immune disorders, viral infections, and cancer.[6] However, the short *in vivo* half-life of IFNγ limits its clinical application. It has been reported that the half-life of IFNγ in humans is about 30 minutes and 4.5 hours after intravenous and intramuscular injection, respectively.[7]

IFNγ gene therapy is a viable approach to maintain the concentration of IFNγ for a long period. In the previous studies, we demonstrated that the duration of transgene expression can be extended by reducing the number of unmethylated CpG dinucleotides in the plasmid DNA (pDNA) backbone[8,9] or by selecting a human ROSA26 promoter or other sustainable promoters.[10] We also showed that sustained IFNγ expression effectively inhibited tumor metastasis[8,9] and reduced the development and progression of atopic dermatitis in mouse models.[11,12]

The ubiquitous expression of IFNγ receptors also greatly limits the therapeutic application of IFNγ, but controlling the tissue distribution of IFNγ could solve this problem. We demonstrated in a previous study that genetically fusing murine serum albumin (MSA) to IFNγ greatly increased the retention of IFNγ in the systemic circulation.[13] The use of any proteins, protein domains, or peptides that have high affinity for target cells for the design of IFNγ fusion protein would be a promising approach to reduce the adverse effects of IFNγ.

Designing IFNγ fusion proteins with a high affinity for cell surface glycosaminoglycans will limit their distribution close to the cells transduced and reduce the level of IFNγ in the systemic circulation. Some proteins are anchored to the cell surface through the interaction with heparan sulfate and the heparin-binding domain (HBD) of such proteins. For example, murine extracellular superoxide dismutase (EC-SOD) has an HBD of the amino acid sequence RKKRRR on the C-terminal and binds to the extracellular matrix through the interaction with glycosaminoglycans, such as heparin and heparan sulfate.[14] In this study, we selected the HBD of EC-SOD and designed IFNγ fusion proteins with one to three HBDs (IFNγ-HBD) to limit their distribution to the region near the site of gene transfer. To prove the availability and usefulness of this strategy, we constructed plasmids encoding IFNγ-HBD fusion proteins and delivered them to mouse liver by the hydrodynamic gene transfer method. The therapeutic and adverse effects of gene delivery of IFNγ-HBD were assessed by examining hepatic metastasis of cancer cells, and loss of body weight and the production of interleukin (IL) 12, respectively.

[1]Department of Biopharmaceutics and Drug Metabolism, Graduate School of Pharmaceutical Sciences, Kyoto University, Sakyo-ku, Kyoto, Japan; [2]Department of Molecular Microbiology, Graduate School of Pharmaceutical Sciences, Kyoto University, Sakyo-ku, Kyoto, Japan. Correspondence: Y Takakura (takakura@pharm.kyoto-u.ac.jp)
Received 31 March 2014; accepted 2 May 2014

RESULTS

IFNγ-HBD fusion proteins bind to the cell surface after being secreted from transfected cells

One, two, or three repeats of the HBD of EC-SOD (RKKRRR) were genetically fused to the C-terminal of IFNγ to obtain IFNγ-HBD_1, IFNγ-HBD_2, and IFNγ-HBD_3, respectively. We used the pcDNA3 plasmid backbone to construct plasmid vectors expressing IFNγ-HBD_n (n = 1, 2, 3) for *in vitro* studies. Figure 1a shows the schematic images of plasmids encoding IFNγ or IFNγ-HBDs. African green monkey kidney COS-7 cells were transfected with each plasmid, and the amounts of IFNγ and IFNγ-HBDs in culture media and cell lysates were measured 24 hours after transfection. The concentration of IFNγ-HBD fusion proteins in the culture media of the cells transfected with pCMV-IFNγ-HBD_1, pCMV-IFNγ-HBD_2, or pCMV-IFNγ-HBD_3 was much lower than the concentration of IFNγ in the media of the cells transfected with pCMV-IFNγ (Figure 1b). Western blot analysis of the culture media of the cells transfected with pCMV-IFNγ showed a single band of around 35 kDa, which is consistent with the molecular weight of IFNγ homodimer (Figure 1c, lane 1). The culture media of cells transfected with pCMV-IFNγ-HBD_1, pCMV-IFNγ-HBD_2, or pCMV-IFNγ-HBD_3 showed a band with a molecular weight slightly higher than 35 kDa (Figure 1c, lanes 2–4), suggesting that the fusion proteins designed are expressed in the cells after transfection.

To confirm whether IFNγ-HBD fusion proteins bound to heparan sulfate, IFNγ-HBD fusion proteins were added to the heparan-immobilized culture plate (Figure 1d). The amount of IFNγ-HBD_2 and IFNγ-HBD_3 bound to heparan sulfate increased as the IFNγ concentration increased, whereas the binding ability of IFNγ and IFNγ-HBD_1 was smaller than IFNγ-HBD_2 and IFNγ-HBD_3. These results suggest that IFNγ-HBD_2 and IFNγ-HBD_3 strongly interacted with heparan sulfate.

To visualize the cellular localization of IFNγ and IFNγ-HBD fusion proteins, immunofluorescent staining of COS-7 cells was performed using anti-IFNγ antibody (Figure 2a). To detect IFNγ and IFNγ-HBD fusion proteins both inside and outside the cells, cells were treated with 0.1% Triton X-100 to permeabilize the cell membrane. Strong IFNγ signals were observed in all the cells transfected with any plasmid. When the cells were not treated with 0.1% Triton X-100, no significant signals were detected in the cells transfected with pCMV-IFNγ, whereas positive signals were detected in the cells transfected with pCMV-IFNγ-HBD_1, pCMV-IFNγ-HBD_2, or pCMV-IFNγ-HBD_3. In addition, these localization of IFNγ-HBDs on cell surface were observed in other two types of cells, mouse embryonic fibroblast cell line NIH 3T3 and human hepatocellular carcinoma cell line HepG2 (data not shown).

To quantitatively evaluate the amount of IFNγ-HBD fusion proteins on the cell surface, flow cytometry was performed after the transfection with pCMV-IFNγ or pCMV-IFNγ-HBD_n (Figure 2b). As a result, finding similar to the immunofluorescent staining experiment was obtained by flow cytometry. When the cells were not treated with 0.1% Triton X-100, the fluorescence-positive cells were 5.25, 8.49, 12.8, and 14.3% for the cells transfected with pCMV-IFNγ, pCMV-IFNγ-HBD_1, pCMV-IFNγ-HBD_2, and pCMV-IFNγ-HBD_3, respectively. These results suggested that they bound to the cell surface after secretion.

IFNγ-HBD fusion proteins activate the GAS-dependent luciferase activity in cultured cells

The biological activity of the IFNγ-HBD fusion proteins was examined using mouse melanoma B16-BL6 cells transfected with pGAS-Luc, a plasmid-encoding firefly luciferase under the control of the

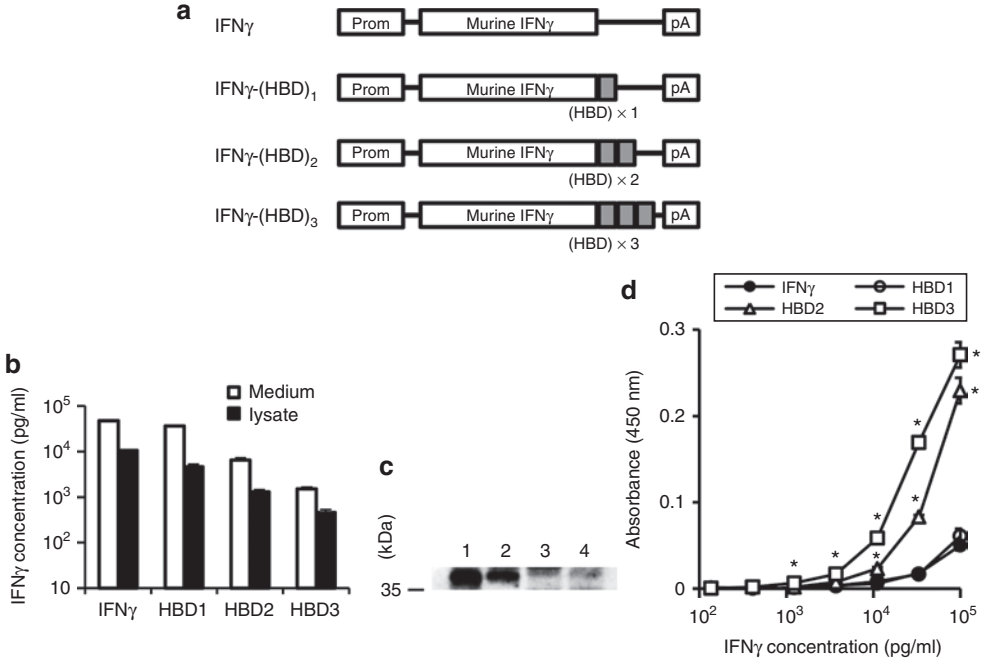

Figure 1 Characteristics of IFNγ-HBD fusion proteins. (**a**) Schematic representation of wild-type and cell surface-interacted interferonγ (IFNγ) genes encoding IFNγ and IFNγ-HBD_1, IFNγ-HBD_2, and IFNγ-HBD_3. (**b**) The concentration of IFNγ in the culture medium of COS7 cells (open column) and cell lysates (solid column) 24 hours after transfection of pCpG-IFNγ and pCpG-IFNγ-HBD_n (0.3 μg/well). Results are expressed as mean ± SEM (n = 3). (**c**) Western blotting analysis of IFNγ-HBD fusion proteins. Lane 1, IFNγ; lane 2, IFNγ-HBD_1; lane 3, IFNγ-HBD_2; and lane 4, IFNγ-HBD_3. (**d**) Heparan sulfate-coating plate was incubated with serial dilutions of IFNγ (solid circles), IFNγ-HBD_1 (open circles), IFNγ-HBD_2 (open triangles), and IFNγ-HBD_3 (open squares) for 2 hours at room temperature. Each protein bound to heparan sulfate was detected by ELISA. Results are expressed as mean ± SEM (n = 3). Asterisk (*) indicates t-test statistically different ($P < 0.05$) from the IFNγ group at the same concentration. ELISA, enzyme-linked immunosorbent assay; HBD, heparin-binding domain; IFN, interferon.

interferon gamma activated site (GAS) (Figure 3). In B16-BL6 cells, the amount of heparan sulfate on the surface of cells is small, because this cell line expresses heparanase, which is a heparan sulfate-degrading enzyme. Therefore, we were simply able to evaluate the biological activities of "free" IFNγ-HBD fusion proteins *in vitro*. Serially diluted IFNγ or IFNγ-HBD fusion proteins collected from culture media of COS-7 cells were added to each well of B16-BL6 cells transfected with pGAS-Luc. The addition of IFNγ increased the luciferase activity in a concentration-dependent manner. The fusion proteins also increased the activity, but the increase was a little smaller than that by IFNγ. The half maximal effective concentration (EC_{50}) values calculated from the dose–response curves were 66.0, 80.5, 81.7, and 83.6 pg/ml for IFNγ, IFNγ-HBD_1, IFNγ-HBD_2, and IFNγ-HBD_3, respectively.

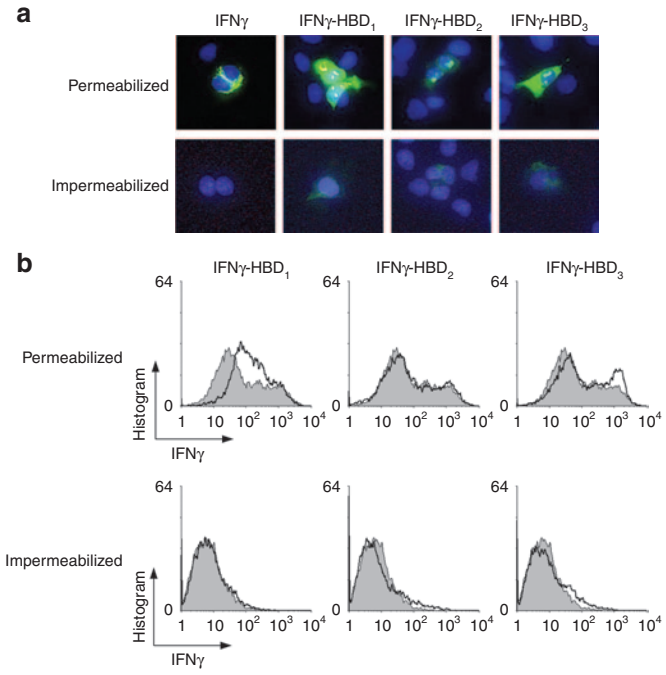

Figure 2 IFNγ-HBD fusion proteins are localized on the cell surface. (**a**) COS-7 cells transfected with IFNγ or IFNγ-HBD fusion proteins expressing pDNA were fixed and stained with monoclonal antibodies against IFNγ, and the cell nuclei were stained with 4′, 6-diamidino-2-phenylindole (blue). The cells were additionally permeabilized with 0.1% TritonX-100 (top) or not (bottom) before staining. Green signals represent IFNγ. (**b**) COS-7 cells transfected with IFNγ (closed area) or IFNγ-HBD fusion proteins (open area) expressing pDNA were fixed and stained with monoclonal antibodies against IFNγ. The amounts of IFNγ both inside and outside the cells were measured by flow cytometry. The cells were additionally permeabilized with 0.1% TritonX-100 (top) or not (bottom) before staining. The result of IFNγ is shown in all the graphs. HBD, heparin-binding domain; IFN, interferon.

Liver-directed gene transfer of IFNγ-HBD fusion proteins increases SOCS1 and γ-IP10 mRNA expression in mouse liver

pCpG vectors were used instead of pcDNA3 vectors for animal studies, because the former are more efficient in terms of transgene expression than the latter in mice. Mice received a hydrodynamic injection of any of the plasmids at different doses, and the livers were harvested 3 days after injection. Figure 4 shows the mRNA expression of IFNγ (or IFNγ-HBD fusion proteins), a suppressor of cytokine signaling 1 (SOCS1), and IFNγ inducible protein 10 (γ-IP10) in the mouse liver. The mRNA expression of the transgenes was dose dependent in all the groups and did not differ markedly from one to the other. The expression of IFNγ significantly increased the mRNA expression of SOCS1 and γ-IP10, indicating that IFNγ expressed in the liver is biologically active. The expression of these genes in the pCpG-IFNγ-HBD_1–injected group was increased to a similar level in the pCpG-IFNγ–injected group. On the other hand, the expression in the pCpG-IFNγ-HBD_2– and pCpG-IFNγ-HBD_3–injected groups was significantly lower than that in the pCpG-IFNγ– or pCpG-IFNγ-HBD_1–injected group, and the mRNA expression in the pCpG-IFNγ-HBD_3–injected group was almost negligible over the dose range examined.

Heparin injection increases the serum concentration of IFNγ-HBD_2 alone

The serum concentration of the transgenes was measured in mice after hydrodynamic injection of pCpG-IFNγ, pCpG-IFNγ-HBD_1, or pCpG-IFNγ-HBD_2 (Figure 5a). pCpG-IFNγ-HBD_3 was not included in this study because IFNγ-HBD_3 hardly induced SOCS1 and γ-IP10 in the mouse liver (Figure 4). As reported in our previous paper, a sustained serum concentration of IFNγ was obtained after injection of pCpG-IFNγ. The levels of serum IFNγ-HBD_1 detected were similar to those of IFNγ. On the other hand, the serum concentrations of IFNγ-HBD_2 were much lower than those of the other two, and they fell below the detection limit 3 days after injection.

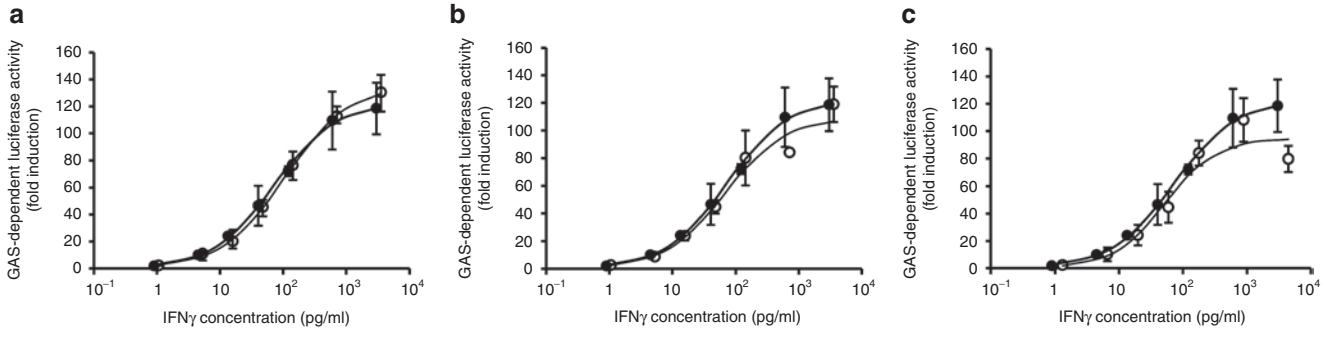

Figure 3 Biological activities of IFNγ-HBD fusion proteins. B16-BL6 cells transfected with pGAS-Luc and phRL-TK were incubated with serial dilutions of IFNγ (solid circles) and IFNγ-HBD fusion proteins (open circles) for 24 hours. pGAS-Luc expressed firefly luciferase under the control of the interferon gamma activated site was used to evaluate the IFNγ activities. phRL-TK expressed renilla luciferase was used to be normalized of transfection efficiencies and cell numbers. The result of IFNγ is shown in all the graphs. (**a**) IFNγ-HBD_1, (**b**) IFNγ-HBD_2, (**c**) IFNγ-HBD_3. The ratio was normalized to give x-fold values relative to those of the untreated group and the half maximum effective concentration (EC_{50}) of each protein was calculated. Results are expressed as mean ± SEM ($n = 3$). GAS, interferon gamma activated site; HBD, heparin-binding domain; IFN, interferon.

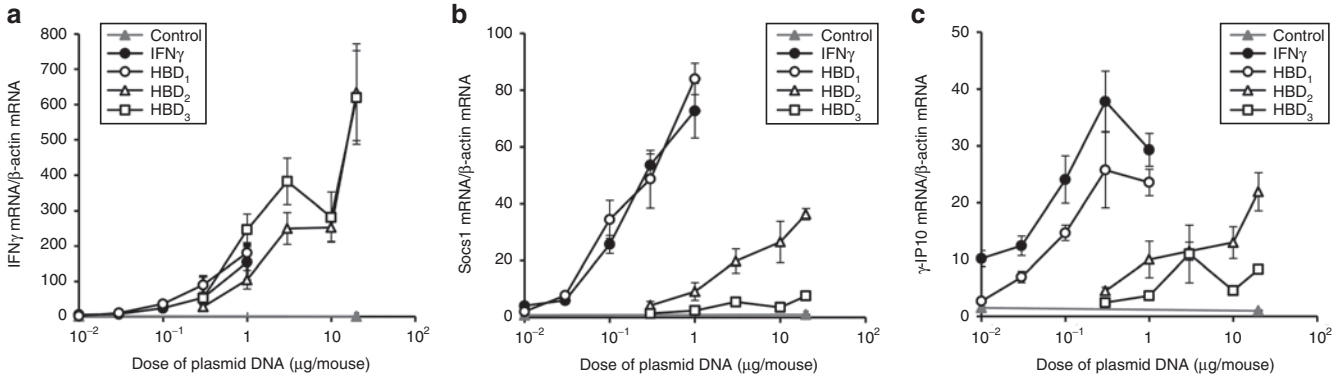

Figure 4 Dose-dependent IFNγ expression and IFNγ induced gene expression in mouse liver. ICR mice were injected with different doses of pCpG-IFNγ (solid circles), pCpG-IFNγ-HBD_1 (open circles), pCpG-IFNγ-HBD_2 (open triangles), and pCpG-IFNγ-HBD_3 (open squares) by hydrodynamic gene transfer. Three days after gene transfer, mice were sacrificed and the livers were collected. (**a**) The mRNA expression of IFNγ, (**b**) The mRNA expression of SOCS1, (**c**) The mRNA expression of γ-IP10. Results are expressed as mean ± SEM (n = 3 or 4). HBD, heparin-binding domain; ICR, Institute of Cancer Research; IFN, interferon.

Three days after injection, the mice injected with any of the plasmids received a heparin injection, and the serum concentration of IFNγ, IFNγ-HBD_1, and IFNγ-HBD_2 was then measured. The serum concentration of IFNγ-HBD_2 was greatly increased (by about 20-fold) by the heparin injection, whereas that of the others remained almost unchanged.

A significant difference in the sensitivity to heparin treatment between IFNγ-HBD_1 and IFNγ-HBD_2 suggests that the length of the HBD peptides is critical for the binding of these fusion proteins to the cell surface. Then, we designed IFNγ-HBD_{1-n} (n = 1, 2, 3, 4, or 5) and IFNγ fusion proteins with the single HBD and additional amino acids of the HBD (Figure 5c). Figure 5d shows the serum concentration of IFNγ-HBD fusion proteins in pCpG-IFNγ-HBD_1, pCpG-IFNγ-HBD_2, or pCpG-IFNγ-HBD_{1-n} (n = 1, 2, 3, 4, and 5) injected mice before and 5 minutes after heparin injection. The serum concentration of IFNγ-HBD fusion proteins tended to increase following heparin injection in all the cases examined, and a positive correlation was observed between the increase in the serum concentration and the number of additional amino acids (Figure 5d,e). However, the increase in IFNγ-HBD_2 was much greater than that in IFNγ-$HBD_{1\text{-}5}$, which is only one amino acid shorter than IFNγ-HBD_2.

Gene delivery of IFNγ-HBD_2 inhibits hepatic metastasis with fewer unwanted side effects

Finally, we evaluated the therapeutic and unwanted side effects after gene delivery of IFNγ and IFNγ-HBD_2. Mice received the low doses of pDNA (0.12 μg/mouse for pCpG-IFNγ and 10 μg/mouse for pCpG-IFNγ-HBD_2) or the high doses of pDNA (0.3 μg/mouse for pCpG-IFNγ and 100 μg/mouse for pCpG-IFNγ-HBD_2) or control pDNA (pCpG-huIFNγ). The serum concentrations of IFNγ in the pCpG-IFNγ and the pCpG-IFNγ-HBD_2 groups were similar tendency to Figure 5a (Figure 6a). Figure 6e shows the number of metastatic colonies of mouse ovarian sarcoma M5076 cells on the liver surface 14 days after inoculation into the tail vein. Injection of 0.12 and 0.3 μg pCpG-IFNγ reduced the number of the colonies to 53 and 49%, respectively, compared to that in the control pDNA-injected group. Injection of 10 and 100 μg pCpG-IFNγ-HBD_2 reduced the number of the colonies to about 56 and 39%, respectively, compared to that in the control pDNA-injected group (Figure 6d,e). Significant inhibitory effect was obtained in the 100 μg pCpG-IFNγ-HBD_2–injected group compared with the control pDNA-injected group. No significant difference was detected between the numbers of any pCpG-IFNγ and any pCpG-IFNγ-HBD_2 groups. Then, the serum concentration of IL 12 p40 and the body weight were measured as indicators of the nonspecific, unwanted side effects of IFNγ. The serum concentration of IL12 p40 was increased by the injection of each dose of pCpG-IFNγ (Figure 6b). In contrast, injection of pCpG-IFNγ-HBD_2 induced less serum concentration of IL12 p40 compared to that of pCpG-IFNγ. Figure 6c shows the body weight of the mice. Again, a significant body weight loss was observed in the 0.12 μg pCpG-IFNγ–injected group, the 0.3 μg pCpG-IFNγ-injected group, and the 100 μg pCpG-IFNγ-HBD_2 but not in the 10 μg pCpG-IFNγ-HBD_2–injected group. In addition, one mouse receiving 0.3 μg pCpG-IFNγ was died during the experimental period.

DISCUSSION

IFNγ exerts its biological activity by binding to IFNγ receptors,[15] which are expressed on a variety of cell types.[16] Therefore, sustained delivery of IFNγ will not be sufficient to increase its therapeutic index, and controlled delivery to target cells is required. To control the tissue distribution of protein drugs, small peptides that bind to target cell surface proteins, such as growth factor receptors[17] and cell adhesion molecules,[18,19] were used to design fusion proteins. In this study, we designed IFNγ-HBD fusion proteins to limit the distribution of IFNγ to the surface of transected cells through the interaction with heparan sulfate glycosaminoglycans. This strategy of the limited distribution of IFNγ was strongly dependent on liver-specific gene transfer by hydrodynamics-based procedure. The liver was selected as a target organ, because IFNγ can be a therapeutic treatment for liver fibrosis, hepatocellular carcinoma, and chronic hepatitis C.

A major concern with fusion proteins is the reduction in biological activity, as demonstrated in our previous study with IFNγ-MSA, IFNγ fused with MSA to the carboxyl-terminal end; it possessed only about 1/200 the biological activity of IFNγ.[13] Szente *et al.*[20,21] demonstrated that the carboxyl-terminal of IFNγ is important for the interaction with its receptor and following intracellular signaling, such as antiviral responses and major histocompatibility complex class II expression. The experimental results of GAS reporter assay showed that all the IFNγ-HBD fusion proteins designed have comparable biological activities to IFNγ, suggesting that the steric hindrance of HBD is much lower than that of MSA (Figure 3).

To our surprise, the expression of IFNγ-HBD fusion proteins was quite dependent on the number of HBD on the fusion proteins. The mRNA expression of the transgenes and IFNγ-inducible genes, SOCS1, and γ-IP10, strongly suggests that the longer peptide

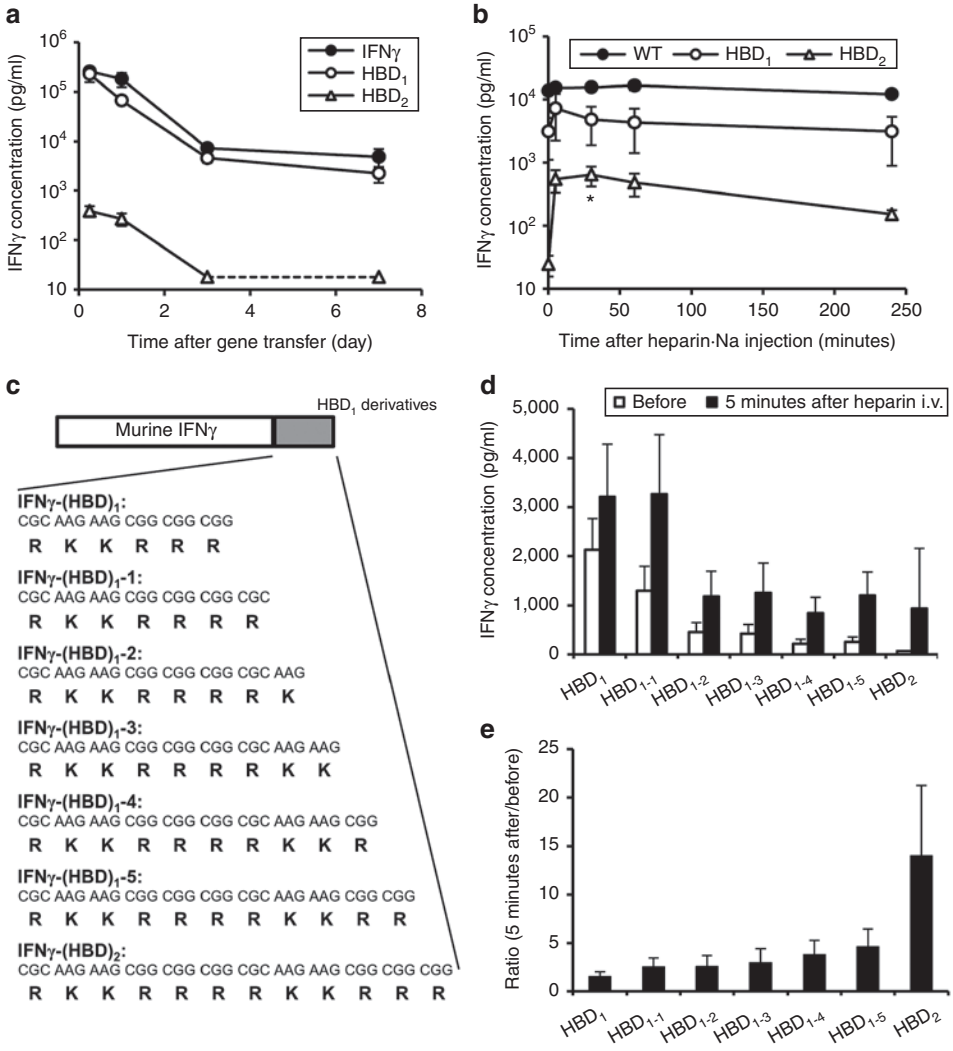

Figure 5 Effect of the level of serum IFNγ-HBD fusion proteins after intravenous injection of heparin. (**a**) Time-course of serum IFNγ concentration in ICR mice after injection of IFNγ-expressing pDNA at a dose of 0.5 μg pDNA/mouse; pCpG-IFNγ (solid circles), pCpG-IFNγ-HBD_1 (open circles), pCpG-IFNγ-HBD_2 (open triangles). Blood samples were collected at the indicated times. Results are expressed as mean ± SEM ($n = 4$). (**b**) 3 days after gene transfer of IFNγ-expressing pDNA at a dose of 0.5 μg pDNA/mouse; pCpG-IFNγ (solid circles), pCpG-IFNγ-HBD_1 (open circles), pCpG-IFNγ-HBD_2 (open triangles), 4000 IU/kg body weight of heparin was injected intravenously into ICR mice. Results are expressed as mean ± SEM ($n = 3$ or 4). Asterisk (*) indicates *t*-test statistically different ($P < 0.05$) from the 0 minute group. (**c**) Schematic representation of IFNγ-HBD_1 derivatives, IFNγ-$HBD_{1\text{-}1}$, IFNγ-$HBD_{1\text{-}2}$, IFNγ-$HBD_{1\text{-}3}$, IFNγ-$HBD_{1\text{-}4}$, IFNγ-$HBD_{1\text{-}5}$. (**d**) 3 days after gene transfer of IFNγ-expressing pDNA at a dose of 5 μg pDNA/mouse; pCpG-IFNγ-HBD_1, pCpG-IFNγ-$HBD_{1\text{-}1}$, pCpG-IFNγ-$HBD_{1\text{-}2}$, pCpG-IFNγ-$HBD_{1\text{-}3}$, pCpG-IFNγ-$HBD_{1\text{-}4}$, pCpG-IFNγ-$HBD_{1\text{-}5}$, pCpG-IFNγ-HBD_2, 4000 IU/kg body weight of heparin was injected intravenously into ICR mice. The serum concentration of IFNγ in mice before (open column) and 5 minutes after intravenous heparin injection (solid column). Results are expressed as mean ± SEM ($n = 4$). (**e**) Analysis of the effect of heparin injection. The ratio was calculated by dividing the serum concentration of IFNγ 5 minutes after heparin injection by that before heparin injection. Results are expressed as mean ± SEM ($n = 4$). HBD, heparin-binding domain; ICR, Institute of Cancer Research; IFN, interferon.

interferes with the expression of fusion proteins in mouse liver (Figure 4b,c). This speculation is supported by the *in vitro* experiments using COS-7 cells, in which the amounts of the transgene products significantly decreased with an increase in the number of HBD fused to IFNγ (Figure 1b).

Heparin injection has been used to confirm the binding of proteins, such as EC-SOD and xanthine oxidase, to glycosaminoglycans.[22,23] Our data showed that an HBD of EC-SOD is not sufficient to restrict IFNγ-HBD fusion protein to the cell surface, and two HBDs are required (Figures 1d and 5b). EC-SOD exists in monomeric, dimeric, or tetrameric forms. It has been reported that the affinity of EC-SOD for heparan sulfate was dependent on the degree of oligomerization, and EC-SOD tetramers were released into the systemic circulation following heparin injection.[22] These properties of EC-SOD would explain the sensitivity to heparin injection or, in other words, binding to the cell surface of IFNγ-HBD_1, IFNγ-HBD_2, and IFNγ-$HBD_{1\text{–}n}$. Taken together with the expression data, we conclude that IFNγ-HBD_2 is an excellent fusion protein with a good balance between binding affinity for heparin sulfate glycosaminoglycans and expression efficiency.

The mRNA expression of the IFNγ-inducible genes in the liver indicates that IFNγ-HBD_2 actually binds to the IFNγ receptors on hepatocytes. This would be largely due to the properties of the hydrodynamic injection method, by which more than 99% of transgene expression was detected in the liver. However, the number of gene-transferred cells was ~10% in the liver after hydrodynamic gene transfer. Therefore, this low gene delivery limited the opportunity for IFNγ-HBD to work in the whole liver. In fact, all IFNγ-HBD fusion

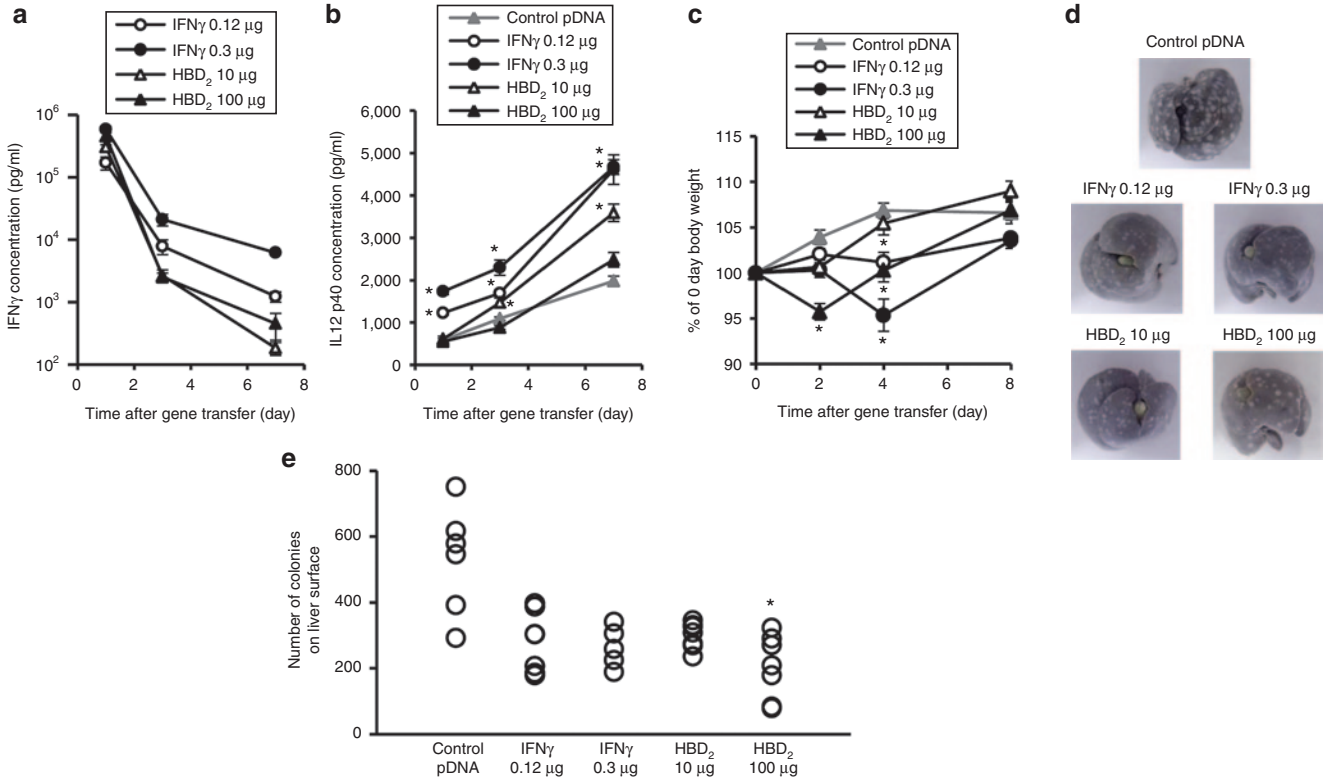

Figure 6 Therapeutic effect of IFNγ-HBD_2 liver-directed gene transfer on the hepatic metastasis of M5076 cells. Hepatic metastasis was established by injection of 1×10^4 M5076 cells into the tail vein of C57BL/6 mice. Three days after implantation of M5076 cells, 0.12 μg pDNA/mouse pCpG-IFNγ (open circles), 0.3 μg pDNA/mouse pCpG-IFNγ (solid circles) 10 μg pDNA/mouse pCpG-IFNγ-HBD_2 (open triangles), 100 μg pDNA/mouse pCpG- IFNγ-HBD_2 (solid triangles) and 100 μg pDNA/mouse pCpG-huIFNγ as control pDNA (closed triangles) was injected by hydrodynamic gene transfer. (**a**) Time-course of the serum concentration of IFNγ after hydrodynamic gene transfer of IFNγ-expressing pDNA. Results are expressed as mean ± SEM ($n = 7$ or survived mice). (**b**) Time-course of the serum concentration of IL12 p40 after hydrodynamic gene transfer of pDNAs. Results are expressed as mean ± SEM ($n = 7$ or survived mice). Asterisk (*) indicates Steel-Dwass test statistically different ($P < 0.05$) from the control pDNA group. (**c**) Time-course of the body weight of mice after hydrodynamic gene transfer of pDNAs. Results are expressed as mean ± SEM ($n = 7$ or survived mice). Asterisk (*) indicates *Steel-Dwass* test statistically different ($P < 0.05$) from the control pDNA group. (**d, e**) 14 days after implantation of M5076 cells, mice were sacrificed. (**d**) Photographs of the livers after inoculation of M5076 cells, (**e**) the number of metastatic colonies on the liver surface was assessed. Results are expressed as mean ± SEM ($n = 7$ or survived mice). Asterisk (*) indicates Steel-Dwass test statistically different ($P < 0.05$) from the control pDNA group. HBD, heparin-binding domain; IFN, interferon.

proteins showed similar biological activities to IFNγ *in vitro* (Figure 3), whereas *in vivo* biological activities of IFNγ-HBD_2 and IFNγ-HBD_3 were less than IFNγ after hydrodynamic gene transfer (Figure 4). We speculate that this inconsistency between *in vitro* and *in vivo* experiments was derived from the amount of heparan sulfate. In the liver, the intercellular space is abundant with tissue matrix including glycosaminoglycan. We considered that IFNγ-HBD_2 showed limited distribution near the transfected cells in the liver, whereas secreted IFNγ distributed to the whole liver. Therefore, IFNγ activity of the whole liver was decreased because the number of hepatocytes that was affected by IFNγ-HBD_2 was less than that of IFNγ. Dedieu *et al.*[24] has shown that adenovirus vector transfected ~80% of hepatocytes in the liver. Therefore, we considered that using adenovirus vector would improve the efficacy of IFNγ-HBD. The inhibition of the proliferation of M5076 cells in the liver also suggested that a therapeutic level of biologically active IFNγ-HBD_2 is limited in the organ.

High concentrations of IFNγ in the systemic circulation result in several adverse events both in humans and mice, including anorexia and weight loss.[25] These adverse events are induced directly by IFNγ[26] or indirectly[27,28] through the up-regulation of other cytokines, including IL12. Following stimulation with IFNγ, IL12 is produced by dendritic cells,[29] macrophages,[30] and B cells.[31] The minor changes in the body weight and IL12 suggest that IFNγ-HBD_2 is delivered in very small amounts to these immune cells after liver-directed gene transfer. The limited production of IL12 is very important for achieving liver-selective delivery of IFNγ fusion proteins, because it is a strong inducer of IFNγ.[32] In addition, death of mice was observed after high dose of pCpG-IFNγ administration. However, in the case of pCpG-IFNγ-HBD_2, no mice died. This result also suggested that fusing HBD to IFNγ is effective to reduce the adverse effect of IFNγ.

In conclusion, we demonstrated that fusing HBD to IFNγ can be used to control the tissue distribution of IFNγ and that the liver-specific distribution of IFNγ obtained by liver-directed gene transfer of IFNγ-HBD_2 is effective in reducing secondary unwanted effects without reducing the therapeutic effect.

MATERIALS AND METHODS

pDNA construction

pCpG-huIFNγ encoding human IFNγ and pCpG-IFNγ-encoding murine IFNγ were constructed as described previously. pCpG-IFNγ-HBD_n (n = 1, 2, 3) were constructed by inserting the polymerase chain reaction (PCR) amplification encoding IFNγ-HBD_n (forward primer: 5′- GAA GAT CTC GGC CTA GCT CTG AGA CAA -3′ and reverse primer: 5′- CTA GCT AGC TCA (CCG CCG CCG CTT CTT GCG)$_n$ GCA GCG ACT CCT TTT CCG CTT -3′) into the *Bgl*II/*Nhe*I site (Figure 1a) of pCpG-mcs vector (InvivoGene, San Diego, CA). pCMV-IFNγ-HBD_n (n = 1, 2, 3) were constructed by inserting the BglII/NheI IFNγ-HBD_n cDNA fragment from pCpG-IFNγ-HBD_n into the *Bam*HI/*Xba*I site of pcDNA3 vector (Invitrogen, Carlsbad, CA). The pGAS (gamma-activated

sequence)-Luc encoding firefly luciferase under the control of the gamma-activated sequence was constructed as described previously. phRL-TK was purchased from Promega (Madison, WI). All IFNγ-expressing pCpG pDNA were amplified in the GT115 of *Esherichia coli*. The other pDNAs were amplified in the DH5α strain of *E. coli*. All pDNA were purified using the JETSTAR 2.0 Plasmid GIGA Plasmid purification Kits (GENOMED, Löhne, Germany). The level of lipopolysaccharide was under the 0.01 EU/ μg pDNA in all pDNA.

Cell culture

A murine melanoma cell line B16-BL6 was obtained from the Cancer Chemotherapy Center of the Japanese Foundation for Cancer Research (Tokyo, Japan). An African green monkey kidney fibroblast cell line COS-7 was obtained from American Type Culture Collection (Manassas, VA). B16-BL6 and COS-7 cells were cultured in Dulbecco's modified Eagle's minimum essential medium (Nissui Pharmaceutical, Tokyo, Japan) supplemented with 10% fetal bovine serum and penicillin/streptomycin/L-glutamine at 37 °C and 5% CO_2. An ovarian sarcoma cell line M5076 was provided by Dr. Yamori (Cancer Chemotherapy Center, Japanese Foundation for Cancer Research, Tokyo, Japan). For animal passage, M5076 cells were i.p. transplanted into the C57BL/6 mice at 5×10^5 cells/animal. The ascites cells were collected 14 days after transplantation.

Transfection

Before the day of transfection, cells were seeded on culture plates. After an overnight incubation, transfection of pDNA was performed utilizing Lipofectamine 2000 (Invitrogen) according to the manufacturer's instructions. In brief, pDNA/Lipofectamine 2000 complexes were prepared in a ratio of 1 μg pDNA/3 μl LA2000.

Western blotting

The supernatants of COS-7 cells transfected with pCMV-IFNγ or pCMV-IFNγ-HBD_n were collected 24 hours after transfection. The samples were subjected to 10% sodium dodecyl sulfate–polyacrylamide gel electrophoresis under reducing or nonreducing conditions and transferred to a polyvinylidene fluoride transfer membrane electrophoretically. After blocking with 2% bovine serum albumin, the membrane was probed with rat antimouse IFNγ monoclonal antibody (1:200; Biolegend, San Diego, CA) for 1 hour at room temperature and then allowed to react with goat anti-rat IgG polyclonal antibody conjugated with horseradish peroxidase (1:2,000; R&D System, Minneapolis, MN) for 1 hour at room temperature. The bands were detected by LAS-3000 (Fuji Film, Tokyo, Japan).

Measurement of the binding affinities of IFNγ-HBD fusion proteins to heparan sulfate

Five microgram of heparan sulfate (Sigma-Aldrich, St Louis, MO) was added into each well of 96-well plates at a volume of 100 μl/well for 2 hours at 37 °C. Wells were added with serially diluted supernatants of COS-7 cells transfected with pCMV-IFNγ or pCMV-IFNγ-HBD_n. After incubation for 2 hours at room temperature, each well was washed with phosphate-buffered saline (PBS) −0.05% Tween 20, and proteins bound to heparan sulfate were detected by enzyme-linked immunosorbent assay (ELISA) using antimouse IFNγ antibody (Ready-SET-GO! Murine IFNγ ELISA; eBioscience, San Diego, CA).

Immunofluorescent staining of IFNγ

To visualize IFNγ expression in cultured cells, immunofluorescent staining of IFNγ was carried out. Cells were fixed with 4% paraformaldehyde in PBS 24 hours after transfection. The cell membrane was permeabilized with PBS containing 0.1% Triton X-100 or not before staining. After blocking with 10% fetal bovine serum in PBS, cells were incubated with a monoclonal rat antibody against IFNγ (1:300; Biolegend). After washing, Alexa Fluor 488 goat antirat secondary antibody (1:300; Molecular Probes, Invitrogen) was added. Nuclear staining was performed using 4',6-diamidino-2-phenylindole staining solution (100 nmol/l 4',6-diamidino-2-phenylindole in PBS). Slides were prepared using a SlowFade Antifade Kit (Molecular Probes). Images were captured using a fluorescent microscope (BZ-8000; Keyence, Osaka, Japan) and processed for deconvoluted fluorescence imaging.

Flow cytometric analysis of IFNγ on the surface of cells

5×10^5 COS-7 cells seeded on 6-well plates were incubated overnight at 37 °C. The cells were transfected with 1 μg/ml pCMV-IFNγ or pCMV-IFNγ-HBD_n. Cells were washed with PBS twice 24 hours after transfection. The cells were detached from the culture plate using 2 mmol/l ethylenediaminetetraacetic acid-2Na, and fixed with 4% paraformaldehyde in PBS. The cell membrane was permeabilized with PBS containing 0.1% Triton X-100 or not before staining. After blocking with 10% fetal bovine serum in PBS, cells were incubated with a monoclonal rat antibody against IFNγ conjugated with Alexa Fluor 488 (1:200; Biolegend). The fluorescent intensity of cells was analyzed by flow cytometry (FACS Calibur; BD Biosciences, Franklin Lakes, NJ) using a CellQuest software (version 3.1, BD Biosciences).

Measurement of the biological activity of IFNγ-HBD fusion proteins

To confirm whether the IFNγ-HBD_n maintained the biological activities of IFNγ, the conditional media, the supernatant of COS-7 cells transfected pCMV- IFNγ or pCMV- IFNγ-HBD_n, were collected 48 hours after transfection. B16-BL6 cells were seeded at 7×10^5 cells on culture dishes and incubated overnight. Cotransfection of each pGAS-Luc (2.8 μg/ml) and phRL-TK (1.2 μg/ml) was performed. After 4 hours transfection, the culture medium was replaced with fresh medium and incubated overnight. B16-BL6 cells were seeded at 1×10^4 cells on 24-well culture plates and reseeded after 24 hours, then culture medium was replaced with fresh medium containing serial dilutions of conditioned media of COS-7 cells transfected with pCpG-IFNγ or pCpG-IFNγ-HBD_n. After 24 hours of incubation, the cells were lysed with a lysis buffer (PiccageneDual; Toyo Ink, Tokyo, Japan), and lysates were mixed using a luciferase assay kit (PiccageneDual; Toyo Ink). Luciferase activities were quantified with LUMAT LB9507 (EG & G Berthold, Bad Wildbad, Germany).

Animals

Four-week-old male ICR mice (~20 g body weight) and 6-week-old male C57BL/6 mice were purchased from Shizuoka Agricultural Cooperative Association for Laboratory Animals (Shizuoka, Japan). The animals were maintained on a standard food and water diet in a temperature- and light-controlled environment. All protocols for the animal experiments were approved by the Animal Experimentation Committee of Graduate School of Pharmaceutical Sciences of Kyoto University. In the *in vivo* gene transfer study, mice received pDNA by a hydrodynamics-based procedure in which naked pDNA dissolved in saline solution (8% of body weight) was injected into the tail vein over 5 seconds.[33] The heparin wash experiments were performed as follows. Three days after hydrodynamic gene transfer, mice were intravenously injected with a shot of 4000 IU/kg body weight heparin.[22] Blood samples were collected before and at the indicated times after the heparin injection.

mRNA quantification

Total RNA was extracted from ~100 mg liver samples using Sepasol RNA I Super (Nakalai Tesque, Kyoto, Japan). Reverse transcription was performed using a ReverTra Ace qPCR RT kit (TOYOBO, Osaka, Japan), followed by RNaseH treatment (Ribonuclease H; Takara Bio, Otsu, Japan). For quantitative analysis of mRNA expression, a real-time PCR was carried out with total cDNA using KAPA SYBR FAST ABI Prism 2X qPCR Master Mix (Kapa Biosystems, Boston, MA). The oligodeoxynucleotide primers used for amplification were *Ifnγ*-sense: 5′- CGGCACAGTCATTGAAAGCCTA -3′, *Ifnγ*-antisense:5′-GTTGCTGATGGCCTGATTGTC-3′, and *β-actin*-sense:5′-CATCC GTAAAGACCTCTATGC-3′, *β-actin*-antisense:5′-ATGGAGCCACCGATCCACA-3′, and *Ifnγ inducible protein 10(γ-IP10)*-sense: 5′- CCTATGGCCCTCATTCTCAC -3′, *γ-IP10*-antisense: 5′- CCTATGGCCCTCATTCTCAC -3′, and *socs1*-sense: 5′- GTGG TTGTGGAGGGTGAGAT -3′, *socs1* -antisense: 5 ′- CCCAGACACAAGCTGCTACA -3′. Amplified products were detected online via intercalation of the fluorescent dye using the StepOnePlus Real-Time PCR System (Applied Biosystems, Foster City, CA, USA). The fractional cycle number at which the fluorescence passes the threshold (C_T values) was used for quantification using a comparative C_T method.[34] The mRNA expression of the target genes of interest was normalized to the mRNA expression level of β-actin.

Measurement of cytokine concentration

The culture medium and serum of mice were collected at indicated times after the transfection. The murine IFNγ concentration was determined by Murine IFNγ ELISA kits (Ready-SET-GO! Murine IFNγ ELISA; eBioscience). The murine IL12 p40 concentration was determined using a murine IL 12 p40 ELISA kit (OptEIATM sets; Pharmingen, San Diego, CA).

Experimental hepatic metastasis

M5076 cells were suspended in Hanks' balanced salt solution. Cell suspensions containing 1×10^4 M5076 cells in 100 µl Hanks' balanced salt solution were injected into the tail vein of C57BL/6 mice to establish experimental hepatic metastasis. Then, 3 days after inoculation of tumor cells, each pDNA was injected into the tail vein by hydrodynamic gene transfer. pCpG-huIFNγ was used as a control pDNA. Then, 14 days after inoculation of tumor cells, 0.3 ml 10% solution of carbon ink (Huekibokuju, Huekinorikougyo, Osaka, Japan) in PBS was injected.[35] The carbon particles in the ink make the metastatic nodules more visible by rendering the liver black. Thirty minutes after injection of the carbon solution, mice were sacrificed, and their livers were bleached by Fekete's solution,[36] and the number of metastatic nodules on the liver surface was counted.

Statistical analysis

Differences were statistically evaluated by Student's *t*-test or Steel–Dwass test for multiple comparison. A *P* value of less than 0.05 was considered as statistically significant.

CONFLICT OF INTEREST

The authors declare no conflict of interest.

ACKNOWLEDGMENTS

This work was supported by Grants-in-Aid for Scientific Research (B) and for Young Scientists (B) from Japan Society for the Promotion of Science and by a Grants-in-Aid for Research on Hepatitis and BSE from the Ministry of Health, Labor and Welfare of Japan.

REFERENCES

1. Grassegger, A and Höpfl, R (2004). Significance of the cytokine interferon gamma in clinical dermatology. *Clin Exp Dermatol* **29**: 584–588.
2. Ellis, CN, Stevens, SR, Blok, BK, Taylor, RS and Cooper, KD (1999). Interferon-gamma therapy reduces blood leukocyte levels in patients with atopic dermatitis: correlation with clinical improvement. *Clin Immunol* **92**: 49–55.
3. Jang, IG, Yang, JK, Lee, HJ, Yi, JY, Kim, HO, Kim, CW *et al.* (2000). Clinical improvement and immunohistochemical findings in severe atopic dermatitis treated with interferon gamma. *J Am Acad Dermatol* **42**: 1033–1040.
4. Stevens, SR, Hanifin, JM, Hamilton, T, Tofte, SJ and Cooper, KD (1998). Long-term effectiveness and safety of recombinant human interferon gamma therapy for atopic dermatitis despite unchanged serum IgE levels. *Arch Dermatol* **134**: 799–804.
5. Noh, GW and Lee, KY (1998). Blood eosinophils and serum IgE as predictors for prognosis of interferon-gamma therapy in atopic dermatitis. *Allergy* **53**: 1202–1207.
6. Schroder, K, Hertzog, PJ, Ravasi, T and Hume, DA (2004). Interferon-gamma: an overview of signals, mechanisms and functions. *J Leukoc Biol* **75**: 163–189.
7. Foon, KA, Sherwin, SA, Abrams, PG, Stevenson, HC, Holmes, P, Maluish, AE *et al.* (1985). A phase I trial of recombinant gamma interferon in patients with cancer. *Cancer Immunol Immunother* **20**: 193–197.
8. Mitsui, M, Nishikawa, M, Zang, L, Ando, M, Hattori, K, Takahashi, Y *et al.* (2009). Effect of the content of unmethylated CpG dinucleotides in plasmid DNA on the sustainability of transgene expression. *J Gene Med* **11**: 435–443.
9. Kawano, H, Nishikawa, M, Mitsui, M, Takahashi, Y, Kako, K, Yamaoka, K *et al.* (2007). Improved anti-cancer effect of interferon gene transfer by sustained expression using CpG-reduced plasmid DNA. *Int J Cancer* **121**: 401–406.
10. Ando, M, Takahashi, Y, Nishikawa, M, Watanabe, Y and Takakura, Y (2012). Constant and steady transgene expression of interferon-γ by optimization of plasmid construct for safe and effective interferon-γ gene therapy. *J Gene Med* **14**: 288–295.
11. Hattori, K, Nishikawa, M, Watcharanurak, K, Ikoma, A, Kabashima, K, Toyota, H *et al.* (2010). Sustained exogenous expression of therapeutic levels of IFN-gamma ameliorates atopic dermatitis in NC/Nga mice via Th1 polarization. *J Immunol* **184**: 2729–2735.
12. Watcharanurak, K, Nishikawa, M, Takahashi, Y, Kabashima, K, Takahashi, R, Takakura, Y. (2012). Regulation of immunological balance by sustained interferon-γ gene transfer for acute phase of atopic dermatitis in mice. *Gene Ther* **20**: 538–544.
13. Miyakawa, N, Nishikawa, M, Takahashi, Y, Ando, M, Misaka, M, Watanabe, Y *et al.* (2011). Prolonged circulation half-life of interferon γ activity by gene delivery of interferon γ-serum albumin fusion protein in mice. *J Pharm Sci* **100**: 2350–2357.
14. Hjalmarsson, K, Marklund, SL, Engström, A and Edlund, T (1987). Isolation and sequence of complementary DNA encoding human extracellular superoxide dismutase. *Proc Natl Acad Sci USA* **84**: 6340–6344.
15. Aguet, M, Dembić, Z and Merlin, G (1988). Molecular cloning and expression of the human interferon-gamma receptor. *Cell* **55**: 273–280.
16. Valente, G, Ozmen, L, Novelli, F, Geuna, M, Palestro, G, Forni, G *et al.* (1992). Distribution of interferon-gamma receptor in human tissues. *Eur J Immunol* **22**: 2403–2412.
17. Fairbrother, WJ, Christinger, HW, Cochran, AG, Fuh, G, Keenan, CJ, Quan, C *et al.* (1998). Novel peptides selected to bind vascular endothelial growth factor target the receptor-binding site. *Biochemistry* **37**: 17754–17764.
18. Fukuda, MN, Ohyama, C, Lowitz, K, Matsuo, O, Pasqualini, R, Ruoslahti, E *et al.* (2000). A peptide mimic of E-selectin ligand inhibits sialyl Lewis X-dependent lung colonization of tumor cells. *Cancer Res* **60**: 450–456.
19. Craig, R, Cutrera, J, Zhu, S, Xia, X, Lee, YH and Li, S (2008). Administering plasmid DNA encoding tumor vessel-anchored IFN-alpha for localizing gene product within or into tumors. *Mol Ther* **16**: 901–906.
20. Szente, BE and Johnson, HM (1994). Binding of IFN gamma and its C-terminal peptide to a cytoplasmic domain of its receptor that is essential for function. *Biochem Biophys Res Commun* **201**: 215–221.
21. Szente, BE, Soos, JM and Johnson, HW (1994). The C-terminus of IFN gamma is sufficient for intracellular function. *Biochem Biophys Res Commun* **203**: 1645–1654.
22. Adachi, T, Yamada, H, Futenma, A, Kato, K and Hirano, K (1995). Heparin-induced release of extracellular-superoxide dismutase form (V) to plasma. *J Biochem* **117**: 586–590.
23. Adachi, T, Fukushima, T, Usami, Y and Hirano, K (1993). Binding of human xanthine oxidase to sulphated glycosaminoglycans on the endothelial-cell surface. *Biochem J* **289** (Pt 2): 523–527.
24. Dedieu, JF, Vigne, E, Torrent, C, Jullien, C, Mahfouz, I, Caillaud, JM *et al.* (1997). Long-term gene delivery into the livers of immunocompetent mice with E1/E4-defective adenoviruses. *J Virol* **71**: 4626–4637.
25. Kaplan, EH, Rosen, ST, Norris, DB, Roenigk, HH Jr, Saks, SR and Bunn, PA Jr (1990). Phase II study of recombinant human interferon gamma for treatment of cutaneous T-cell lymphoma. *J Natl Cancer Inst* **82**: 208–212.
26. Guy-Grand, D, DiSanto, JP, Henchoz, P, Malassis-Séris, M and Vassalli, P (1998). Small bowel enteropathy: role of intraepithelial lymphocytes and of cytokines (IL-12, IFN-gamma, TNF) in the induction of epithelial cell death and renewal. *Eur J Immunol* **28**: 730–744.
27. Matthys, P, Dijkmans, R, Proost, P, Van Damme, J, Heremans, H, Sobis, H *et al.* (1991). Severe cachexia in mice inoculated with interferon-gamma-producing tumor cells. *Int J Cancer* **49**: 77–82.
28. Marrack, P, Blackman, M, Kushnir, E and Kappler, J (1990). The toxicity of staphylococcal enterotoxin B in mice is mediated by T cells. *J Exp Med* **171**: 455–464.
29. Kaliński, P, Hilkens, CM, Snijders, A, Snijdewint, FG and Kapsenberg, ML (1997). IL-12-deficient dendritic cells, generated in the presence of prostaglandin E2, promote type 2 cytokine production in maturing human naive T helper cells. *J Immunol* **159**: 28–35.
30. Hsieh, CS, Macatonia, SE, Tripp, CS, Wolf, SF, O'Garra, A and Murphy, KM (1993). Development of TH1 $CD4^+$ T cells through IL-12 produced by Listeria-induced macrophages. *Science* **260**: 547–549.
31. Schultze, JL, Michalak, S, Lowne, J, Wong, A, Gilleece, MH, Gribben, JG *et al.* (1999). Human non-germinal center B cell interleukin (IL)-12 production is primarily regulated by T cell signals CD40 ligand, interferon gamma, and IL-10: role of B cells in the maintenance of T cell responses. *J Exp Med* **189**: 1–12.
32. Nastala, CL, Edington, HD, McKinney, TG, Tahara, H, Nalesnik, MA, Brunda, MJ *et al.* (1994). Recombinant IL-12 administration induces tumor regression in association with IFN-gamma production. *J Immunol* **153**: 1697–1706.
33. Liu, F, Song, Y and Liu, D (1999). Hydrodynamics-based transfection in animals by systemic administration of plasmid DNA. *Gene Ther* **6**: 1258–1266.
34. Schmittgen, TD and Livak, KJ (2008). Analyzing real-time PCR data by the comparative C(T) method. *Nat Protoc* **3**: 1101–1108.
35. Lafreniere, R and Rosenberg, SA (1985). Successful immunotherapy of murine experimental hepatic metastases with lymphokine-activated killer cells and recombinant interleukin 2. *Cancer Res* **45**: 3735–3741.
36. Fekete, E (1938). A comparative morphological study of the mammary gland in a high and a low tumor strain of mice. *Am J Pathol* **14**: 557–578.5.